Physics of the Earth and Planetary Interiors 253 (2016) 58–63

Contents lists available at ScienceDirect

Physics of the Earth and Planetary Interiors

journal homepage: www.elsevier.com/locate/pepi

Letter

Tomography of the source zone of the 2015 M 7.8 Nepal earthquake

Wei Wei [a,b,*], Dapeng Zhao [b]

[a] Key Laboratory of Active Tectonics and Volcano, Institute of Geology, China Earthquake Administration, Beijing, China
[b] Department of Geophysics, Tohoku University, Sendai 980-8578, Japan

A R T I C L E I N F O

Article history:
Received 23 August 2015
Received in revised form 28 November 2015
Accepted 22 January 2016
Available online 3 February 2016

Keywords:
Seismic tomography
Seismic anisotropy
Seismotectonics
2015 Nepal earthquake
Himalaya collision belt

A B S T R A C T

We conducted P-wave anisotropic tomography beneath Nepal and surrounding areas to clarify the causal mechanism of the 25 April 2015 Nepal earthquake (Mw 7.8) and dynamic processes of the India-Asia collision zone. Our results show that hypocenters of the 2015 Nepal mainshock and the 1833 Nepal earthquake (M 8.0) are located in a zone with a higher P-wave velocity (high-V), and the high-V zone coincides with the coseismic slip area of the 2015 Nepal mainshock. The high-V zone may reflect a strongly coupled patch (i.e., asperity) in the megathrust zone between the subducting Indian plate and the overlying Eurasian plate. This result suggests that the nucleation of the Nepal earthquakes was controlled by structural heterogeneities in the megathrust zone. Significant variations of P-wave velocity anisotropy are revealed across the Himalaya collision belt. The predominant fast P-wave velocity direction is NE–SW beneath northern India, whereas it becomes NW–SE beneath the Himalaya, suggesting that the fossil anisotropy in the Indian plate is overprinted by the ongoing India-Asia collision.

1. Introduction

On 25 April 2015, a devastating earthquake (Mw 7.8) struck central Nepal, causing more than 8000 deaths and at least twice of the number injured. Its epicenter was located at 28.23°N, 84.731°E by the U.S. Geological Survey (USGS) (http://earthquake.usgs.gov), which was ~80 km northwest of Kathmandu, the capital of Nepal (Fig. 1a). Its rupture initiated at a depth of 15 km, on or near the Main Himalayan Thrust, and propagated toward the east-southeast over a distance of ~160 km with a duration of ~55 s (Fan and Shearer, 2015). Many aftershocks occurred following the main shock, including two major aftershocks (M 6.7 and M 7.3) taking place east of Kathmandu (Fig. 1a). These large Nepalese thrust earthquakes were the direct result of subduction of the Indian plate beneath the Eurasian plate.

The India-Asia collision is one of the most important tectonic events on Earth, which, to date, created the Himalaya and Tibetan Plateau. At present, the convergence rate across the Nepalese Himalaya is ~17–20 mm/year (Ader et al., 2012), which accounts for ~40% of the total India-Asia convergence. This active deformation zone is also the place where great earthquakes occur frequently (Fig. 1a). A big event (M 8.0) on 26 August 1833 occurred north of Kathmandu. The largest earthquake in Nepal in the past century took place on 15 January 1934 with a magnitude of 8.2, which broke the surface over a length of >150 km (Sapkota et al., 2013). The 2015 Nepal earthquake was located to the west of the 1833 and 1934 events (Fig. 1a).

To understand how these large earthquakes were generated, we need to study the structure and mechanical properties of the Main Himalayan Thrust. Previous studies have suggested that the nucleation of megathrust earthquakes in subduction zones is controlled by structural heterogeneities in the megathrust zone (e.g., Zhao et al., 2011; Huang and Zhao, 2013; Liu et al., 2013; Romano et al., 2014; Liu and Zhao, 2014). In this work, we study the 3-D P-wave velocity (Vp) structure and seismic anisotropy in the source zone of the 2015 Nepal earthquake and surrounding areas. Our results provide new information on the causal mechanism of the Nepal earthquakes as well as the dynamic process of continental collision in the Himalayan region.

2. Data and method

In this study, we combined two data sets of local-earthquake arrival times to conduct tomographic inversions. One set of data was recorded by temporary seismic arrays deployed in Nepal and the Tibetan Plateau. The other is selected from the modified Bulletin of the International Seismological Center (Engdahl et al., 1998) for the period of 1991–2008. We selected the P-wave arrival-time data according to the following criteria: (1) each earthquake was recorded by more than 8 seismic stations and has a reliable hypocentral location; (2) each P-wave arrival has a

* Corresponding author at: Key Laboratory of Active Tectonics and Volcano, Institute of Geology, China Earthquake Administration, Beijing, China.

http://dx.doi.org/10.1016/j.pepi.2016.01.008
0031-9201/

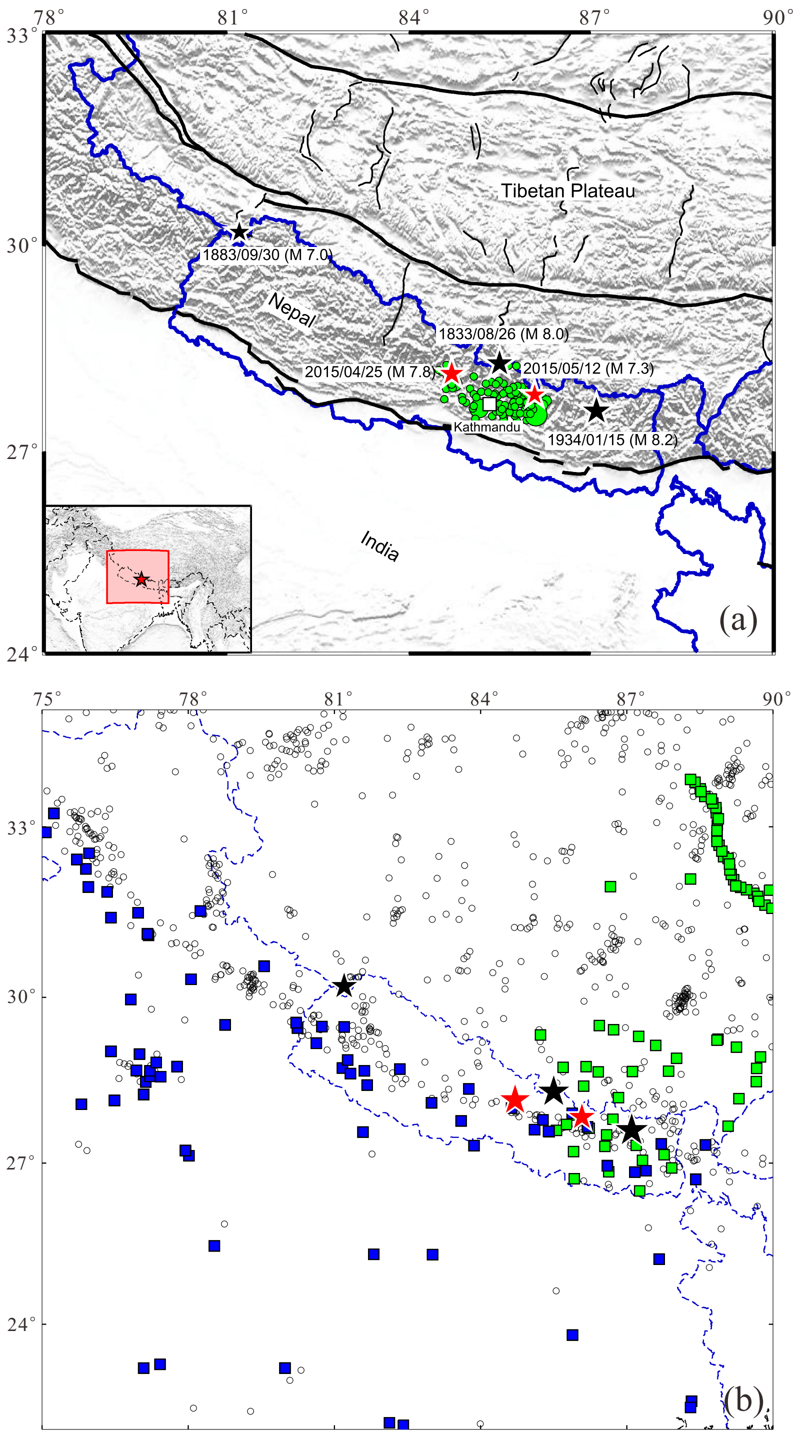

Fig. 1. (a) Tectonic background and topographic relief of the study region. The red and black stars represent large earthquakes with magnitude >7.0 which occurred in Nepal since 1833. The thick black lines show the large active faults and sutures. The green dots denote the aftershocks of the 2015 Nepal earthquake (M 7.8). The white square shows the location of Kathmandu. The blue lines show the national boundaries. The inset map shows the location of the present study region. The red star in the inset map shows the epicenter of the 2015 Nepal earthquake (M 7.8). (b) Distribution of 358 events (open circles) and 135 seismic stations used in this study. The blue and green squares denote the stations compiled by the International Seismological Center (ISC) and temporary seismic experiments, respectively. The two red stars show the epicenters of the 2015 Nepal earthquake (M 7.8) and its largest aftershock (M 7.3). The three black stars show the epicenters of large historic earthquakes (see (a) for details). (For interpretation of the references to color in this figure legend, the reader is referred to the web version of this article.)

picking accuracy of <0.2 s and a travel-time residual less than 2.0 s. As a result, a total of 7092 high-quality P-wave arrival times from 358 well-located local events are selected (Fig. 1b).

We applied the tomographic method of Zhao et al. (1992, 2011) and Wang and Zhao (2008) to analyze our data set for determining P-wave tomography and azimuthal anisotropy. Referring to previous studies of this region (Monsalve et al., 2006; Huang et al., 2009), we adopted the starting one-dimensional Vp model shown in Fig. S1. Because the Moho depth variations can affect significantly ray paths and travel times (e.g., Zhao et al., 1992; Wei et al., 2012), we took into account the topography of the Moho discontinuity in the study region. The Moho depth distribution is shown in Fig. S2, which is inferred from the CRUST 1.0 model (Pasyanos et al., 2014). Two 3-D grid nets are set up in the